

Thermophotonic cooling in GaAs based light emitters ^{EP}

Cite as: Appl. Phys. Lett. **114**, 051101 (2019); <https://doi.org/10.1063/1.5064786>

Submitted: 08 October 2018 . Accepted: 23 December 2018 . Published Online: 05 February 2019

Ivan Radevici, Jonna Tiira, Toufik Sadi, Sanna Ranta ^{id}, Antti Tukiainen ^{id}, Mircea Guina ^{id}, and Jani Oksanen

COLLECTIONS

^{EP} This paper was selected as an Editor's Pick



View Online



Export Citation



CrossMark

ARTICLES YOU MAY BE INTERESTED IN

[Electroluminescent refrigeration by ultra-efficient GaAs light-emitting diodes](#)

Journal of Applied Physics **123**, 173104 (2018); <https://doi.org/10.1063/1.5019764>

[Magneto-mechanical trapping of micro-diamonds at low pressures](#)

Applied Physics Letters **114**, 053103 (2019); <https://doi.org/10.1063/1.5066065>

[Dielectric function and band structure of Sn_{1-x}Ge_x \(x < 0.06\) alloys on InSb](#)

Applied Physics Letters **114**, 062102 (2019); <https://doi.org/10.1063/1.5086742>

Lock-in Amplifiers
up to 600 MHz



Thermophotonic cooling in GaAs based light emitters

Cite as: Appl. Phys. Lett. **114**, 051101 (2019); doi: [10.1063/1.5064786](https://doi.org/10.1063/1.5064786)

Submitted: 8 October 2018 · Accepted: 23 December 2018 ·

Published Online: 5 February 2019






View Online



Export Citation



CrossMark

Ivan Radevici,^{1,a)} Jonna Tiira,¹ Toufik Sadi,¹ Sanna Ranta,²  Antti Tukiainen,²  Mircea Guina,² 
and Jani Oksanen¹

AFFILIATIONS

¹Engineered Nanosystems Group, Aalto University, Aalto 00076, Finland

²Optoelectronics Research Centre, Tampere University of Technology, Tampere 33101, Finland

^{a)}Electronic mail: ivan.radevici@aalto.fi

ABSTRACT

Fundamental thermodynamic considerations reveal that efficient emission from an electrically injected light emitting diode (LED) can lead to the cooling of the device. This effect, known as electroluminescent (EL) cooling, has been identified decades ago, but it has not been experimentally demonstrated in semiconductors at practical operating conditions due to the extreme requirements set for the efficiency of the light emission. To probe the conditions of EL cooling in GaAs based light emitters, we have designed and fabricated LED structures with integrated photodiodes (PDs), where the optically mediated thermal energy transport between the LED and the PD can be easily monitored. This allows characterization of the fundamental properties of the LED and a path for eliminating selected issues encountered in conventional approaches for EL cooling, such as the challenging light extraction. Despite several remaining nonidealities, our setup demonstrates a very high directly measured quantum efficiency of 70%. To characterize the bulk part of the LED, we also employ a model for estimating the power conversion efficiency (PCE) of the LED, without the contribution of non-fundamental nonidealities such as photodetection losses. Our results suggest that the PCE of the LED peaks at around 105–115%, exceeding the 100% barrier required to reach the EL cooling regime by a clear margin. This implies that the LED component in our device is in fact cooling down by transporting thermal energy carried by the emitted photons to the PD. This provides a compelling incentive for further study to confirm the result and to find ways to extend it for practically useful EL cooling.

Published under license by AIP Publishing. <https://doi.org/10.1063/1.5064786>

The basic principles of electroluminescent (EL) cooling and the closely related photoluminescent (PL) cooling of semiconductors have been known for well over half a century.^{6,13,20} In both phenomena, radiative recombination produces photons with an energy larger than the bandgap of the emitting semiconductor, even when the energy used to generate the recombining electron-hole pairs is smaller than the bandgap. The energy difference is provided by heat taken from the crystal lattice enabling, for a suitable combination of external quantum efficiency (EQE) and energy used to generate the electron-hole pairs, refrigeration of the semiconductor.¹⁹ Unlike the efficiency of optical pumping in PL cooling, however, the excitation efficiency by current injection in EL cooling is generally not reduced even when the excitation energy falls well below the bandgap value. Despite this and the considerable improvements in the efficiency of electrically injected light emitting diodes

(LEDs) during the past few decades, the first experimental indications of EL cooling have been reported only very recently but at very small bias voltages ($U < 100 \mu\text{V}$) and EQEs ($\eta_{\text{EQE}} \sim 10^{-4}$), resulting in extremely small cooling powers ($P_c \sim 50 \text{ pW}$),^{16,17} which are too small for most practical applications. Reaching the large bias EL cooling regime with practically useful LED current densities and cooling powers exceeding the A/cm^2 and mW limits, respectively, will require semiconductor devices with a very high quantum efficiency and bias voltages closer to normal LED operating conditions.

To date, the highest reported EQEs for the dominating LED materials at room temperature extend all the way up to 96% for optically pumped GaAs structures⁷ and $\sim 80\%$ – 81% ⁹ and 68%³ for electrically injected GaN and GaAs double heterojunction (DHJ) LEDs, respectively. Despite the presently lower EQE, it is typically expected that the electrically injected GaAs system

provides the most suitable candidate for EL cooling for a number of reasons. These include (i) the substantially larger reported internal quantum efficiencies (IQE), exceeding 99.5%,^{1,18} which is of key importance especially for devices where photons will not be extracted in air; (ii) the mature fabrication technology;⁴ and (iii) the potentially higher cooling rates due to the availability of lattice matched materials, allowing optically thick emitter regions and the larger optical density of states following from the larger refractive index.²

To study EL cooling and the related photon and energy transport effects in GaAs based light emitters in the high power regime in more detail, we recently introduced the double diode structure (DDS) illustrated in Fig. 1(a).¹² The DDS consists of two semiconductor diodes grown within a single epitaxial growth process, essentially forming a thermophotonic (TPX) heat pump system where light extraction is not necessary. The upper diode is a DHJ LED injected by an external current I_1 and voltage U_1 , while the lower diode is a homojunction photodetector (PD) absorbing light from the emitter and producing an external

current I_2 . In reality, however, the thermal conduction between the LED and the PD needs to be reduced for the LED to visibly cool down. This is expected to be possible later on, e.g., by introducing vacuum nanogaps^{4,5,11} or a suitable light extraction system^{7,19} and spatial separation between the LED and the PD as illustrated in Fig. 1(b). As such, the DDS structure is designed to act as an intermediate research prototype for directly probing and optimizing the efficiency and energy transport in the structure using the built-in PD, providing the necessary additional insight and evidence on the feasibility of both conventional EL cooling and thermophotonic cooling.¹⁵

In this paper, we analyze the performance of selected DDSs, showing that the included LED junctions potentially exhibit the highest directly measured quantum efficiencies of GaAs based LEDs. Based on a separate loss analysis, our results additionally suggest that the power conversion efficiency of our LED components already exceeds the threshold of EL cooling by at least 10%. This further suggests that from the fundamental point of view, EL cooling and thermophotonic cooling are feasible and may provide an alternative solid-state cooling technology if suitable thermal insulators can be developed.

The epitaxial structures used for fabricating the DDS were grown by molecular beam epitaxy (MBE). Detailed information about the device layers is given in Fig. 1. A combination of standard lithography steps and selective wet chemical etching was used to define the DDS mesas with LED diameters of 100, 200, 500, and 1000 μm . After forming the double mesa structure, the topmost p-GaAs layer was patterned and partly etched. Then, a silicon nitride layer with contact openings was fabricated on the samples by plasma enhanced chemical vapor deposition (PECVD) before the contact metallization. This was carried out to fabricate omnidirectional reflectors (ODRs) that reduce the optical losses due to absorption by the GaAs layer and the metal contacts. The fabricated ODRs have an area coverage factor varying from 0.05 to 1.00 under the top contact.

The DDS was characterized using a 3 point measurement setup simultaneously biasing the LED and short-circuiting the PD while measuring the LED and PD currents I_1 and I_2 , respectively. To avoid unnecessary heating, all measurements with an LED injection current >100 mA were performed in a pulsed mode with pulses shorter than 1ms and separated by a 2 s delay between them. Overall, the measurement configuration corresponds to an LED with nearly ideal light extraction connected to an external (nonideal) integrating sphere measuring the generated photon flux. The measured currents were used to calculate the coupling quantum efficiency (CQE) of the DDS defined as $\eta_{\text{CQE}} = I_2/I_1$. This value represents the lower limit of the quantum efficiency of the LED because the detected current I_2 for the used PD structure is still substantially smaller than the current corresponding to the photon flux emitted by the LED, e.g., due to additional recombination losses in the presently suboptimal PD. In the DDS context, the CQE corresponds to the EQE of an LED with a light extraction efficiency matching the IQE of the PD.

In the process of characterizing the fabricated DDSs, we measured all the DDS mesas with different area coverages and diameters ranging from 100 to 1000 μm . However, for all the

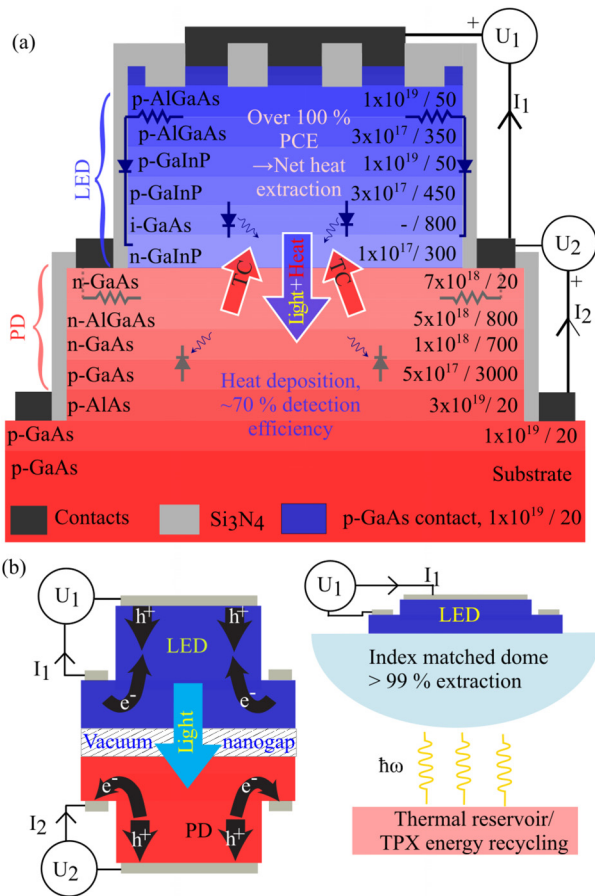


FIG. 1. (a) Schematic representation of the DDS mesa (not in scale) with detailed information about the doping ($1/\text{cm}^3$) and the layer thicknesses (nm). (b) A schematic approach to harness EL cooling in practical devices using vacuum nanogaps or efficient light extraction to reduce thermal conduction.

results discussed below, mesas with a $1000\ \mu\text{m}$ diameter and an area coverage ranging from 0.02 to 0.20 were used as these devices exhibited some of the highest efficiencies.

Figure 2 analyses the electrical characteristics of the DDS using the sample exhibiting the highest value of CQE as an example. In Fig. 2(a), the measured LED and PD current densities (left axis), as well as the corresponding CQE (right axis), are presented on a linear scale as a function of the LED bias. The inset additionally shows the CQE as a function of the current density. The CQE keeps increasing throughout the measurement range and eventually peaks at the value of $\eta_{\text{CQE}} = 0.70$, at a current density of $J = 50\ \text{A}/\text{cm}^2$, and at the edge of the measurement range. The same $J - V$ curves are plotted on a semilogarithmic axis in Fig. 2(b) with a fit to the exponential part of the curves. The electrical characteristics demonstrate the expected exponential diode behaviour up to the bias voltages $\sim 1.2\text{--}1.3\ \text{V}$, after which the resistive losses in the LED and the measurement setup start to dominate. The ideality factors fitted to the exponential parts are 2 and 1 for the LED and the PD, respectively. This shows that Shockley-Read-Hall (SRH) like non-radiative recombination dominates the exponential part in the LED. Similarly, because the photocurrent in the PD is generated as a result of the radiative recombination in the LED, the bimolecular form of the photocurrent in the PD shows that the radiative

recombination in the LED is also mainly bimolecular. From the small current regimes of the $J - V$ curve, it is evident that there is negligible current leakage from the LED to the PD. This conclusion, also verified by extensive simulations, applies equally well in the large bias regime due to the chosen bias conditions and the device structure, excluding any transistor-like crosstalk between the LED and the PD. However, the $J - V$ characteristics of the LED show a clear deviation from the ideal diode curve at around $\sim 1.1\ \text{V}$ before conforming to the typical resistance limited behaviour. To understand the origin of this irregularity, we modeled the electrical characteristics of the LED using the equivalent circuit illustrated in the inset of Fig. 2(c).^{14,15}

The shoulder of the LED's $J - V$ curve observed from experimental data is fully reproducible with the EC in Fig. 2(c). The circuit assumes that the LED current in the real DDS can flow through two possible parallel channels. The first one, presented on the top branch of the EC, describes the surface states at the external mesa edge. This channel can be analyzed as a diode with an ideality factor of 2 and an additional resistance in series describing the lateral transport of holes through the narrow p-doped channel from the edge of the top-contact to the edge of the mesa. The lower current channel represents the LED diode itself.

The current flow through the equivalent circuit diodes can be approximated by the well-known ABC-model^{8,10,21} described in the supplementary material. Since the recombination is mainly SRH-like in diode D_s and radiative in diode D_1 after the current through it becomes comparable with the surface current, the equivalent circuit model reproduces the measured current when we use $R_s = 250\ \Omega$ for the surface resistance, $A_s^{\text{EC}} = 2 \times 10^7\ \text{s}^{-1}$ and $B_s^{\text{EC}} = C_s^{\text{EC}} = 0$ for the surface diode, and $B_1^{\text{EC}} = 2 \times 10^{-16}\ \text{s}^{-1}\text{m}^{-6}$ and $A_1^{\text{EC}} = C_1^{\text{EC}} = 0$ for D_1 . This shows that for the voltages up to $1.1\ \text{V}$, the electrical characteristics of the DDS are dominated by the surface states at the DDS mesa edge. However, at larger voltages and currents, the significance of the surface currents is strongly reduced. In further analysis, we will not assume the above estimates for the ABC parameters of the LED unless specified otherwise.

The $\eta_{\text{CQE}} = 0.70$ reported here exceeds the CQE records ($\eta_{\text{CQE}} = 0.63$) we have reported previously^{14,15} and also slightly exceeds the highest EQE $\eta_{\text{EQE}} = 0.68$ reported for GaAs based LEDs in the literature.³ While directly comparing the EQE of established GaAs LEDs and our devices' CQE is not straightforward, we nevertheless point out that they both provide a lower limit for the IQE; thus, our result increases the directly measured lower bound for the IQE of GaAs based LEDs.³

For further device optimization and better understanding of the physical processes taking place in the DDS, it is important to separately analyze the losses in the LED and the PD parts. Since this is not possible through direct measurements, we estimate the magnitude of the losses using the ABC-model and the equivalent circuit described above, following the widely adopted assumptions used, e.g., for estimating and modeling the IQE of GaAs LEDs. To this end, we define the radiative recombination coupling factor ξ as the ratio between the photocurrent in the PD and the total radiative recombination current in the LED and cast the ABC-model into a form that allows fitting with our

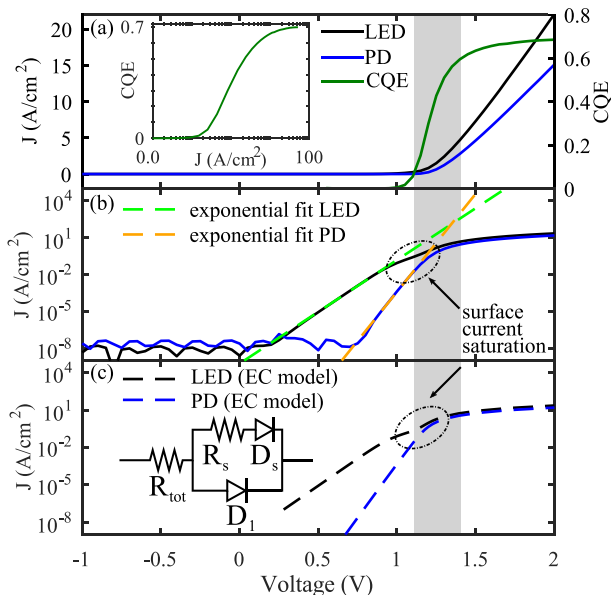


FIG. 2. (a) The measured current density J as a function of the applied LED voltage U_1 for the $1000\ \mu\text{m}$ diameter and 0.2 area coverage DDS LED and PD on a linear scale (left axis) and the corresponding CQE (right axis, plotted only for the range $U_1 > 0.5\ \text{V}$). The inset additionally shows the CQE as a function of the average current density through the LED over the full measurement range. (b) The same $J - U_1$ characteristics plotted on a semilogarithmic scale with a fit to the purely exponential portion of the curve to estimate the diode ideality factors. (c) The equivalent circuit allowing to model the feature on the $J - U_1$ characteristics caused by the surface states and the modelled curves. The shadowed area highlights the region between the GaAs bandgap ($1.42\ \text{eV}$) and the voltage corresponding to 80% of the gap, which would allow cooling with $\eta_{\text{CQE}} = 80\%$.

results, as described in the [supplementary material](#). For the device whose $J - V$ characteristics are presented in [Fig. 2](#), the radiative recombination factor is $\xi = 0.70$, indicating that nearly all losses arise from the photodetection process. However, considering all the fabricated samples, whose CQE ranges between 0.60 and 0.70, the photodetection efficiency is estimated to vary between 0.63 and 0.80.

Taking into account that the CQE is the product of the photodetection and LED quantum efficiencies, we can also estimate the quantum efficiency of the LED component itself as $\eta_{LED} = \eta_{CQE}/\xi$. For the devices with the highest CQEs, this suggests that the quantum efficiency of the LED peaks at very high values approaching unity. This suggests that in terms of the IQE, the best LEDs in the studied DDS structures are estimated to approach unity and are therefore fully comparable with the best previously reported LEDs and PL devices.

In general, a high quantum efficiency alone is not sufficient for reaching the EL cooling regime of a LED. The applied bias must also be low enough for the power conversion efficiency (PCE) to satisfy the condition $\eta_{PCE} = \eta_{QE} \times (\hbar\omega/qU) > 1$, where η_{QE} is the quantum efficiency at which the LED is able to send out photons and U is the real bias voltage over the LED not including the additional external resistive losses arising, e.g., from the measurement setup, which dominates the LED resistance in our case. [Figure 3](#) compares the PCE for 5 different DDS mesas with a 1000 μm diameter and area coverages ranging from 0.02 to 0.20. A photon energy corresponding to the room temperature GaAs bandgap ($\hbar\omega = 1.42 \text{ eV}$), which slightly underestimates the average photon energy, was used for the PCE evaluation. The group of curves labeled “experimental” in the inset of [Fig. 3](#) uses the externally applied bias voltage ($U = U_1$) and the directly measured CQE to calculate the lower limit for the PCE. The curve “normalized by PD efficiency” corrects

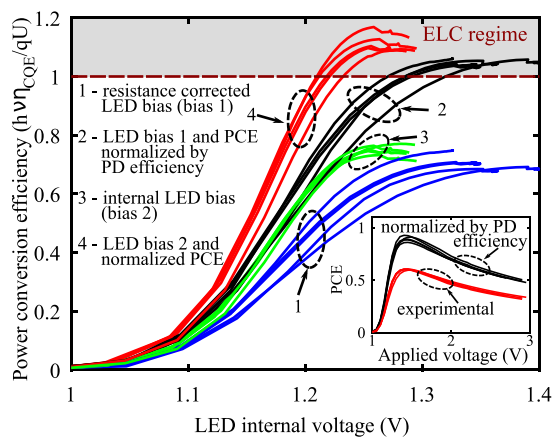


FIG. 3. Power conversion efficiency of the LED as directly evaluated using the measured CQE (curve groups 1, 3, and “experimental” in the inset) and as estimated without the contribution of the photodetection losses (curve groups 2, 4, and “normalized by the PD efficiency”). The curves are plotted as a function of the full applied bias (inset) and the LED bias estimated by elimination of the resistive losses in the measurement setup (curve sets 1 and 2) and by using the PD photocurrent (curve sets 3 and 4). Multiple curves correspond to selected best performing devices. At values above unity, EL cooling takes place.

this PCE by eliminating the losses related to the imperfect photodetection by dividing the experimental PCE by the photodetection efficiency ξ . Curve sets 1–2 in the full figure also use either the directly measured CQE or the CQE corrected by the photodetection efficiency as above to estimate the PCE but with the external bias voltage U_1 replaced by the resistance corrected LED bias $U \approx U_1 - R_{tot}I_1$ instead. In this case, the voltage corresponds to the actual bias of the LED and does not include the ohmic losses associated with the measurement setup and the n-type current spreading layers outside the LED mesa, which are not of fundamental physical importance here and can be mainly eliminated by redesigning the measurement setup and the DDS structure. The series resistance R_{tot} is well approximated by the differential resistance of the LED at large currents (corresponding in the studied case to $R_{tot} \approx 3.95\Omega$) because R_{tot} strongly dominates the differential resistance in this region. Alternatively, and due to the uncertainties in the resistance perhaps more fundamentally, we also use the PD current to estimate the internal LED bias U_{LED} since the PD current is expected to scale as $I_2 = I_{ref} \exp[q(U_{LED} - U_{ref})/kT]$, as long as the carrier densities in the LED remain sufficiently non-degenerate. In our case, we expect that this is the case throughout the measurement regime as the predicted bias voltages remain well below the E_g/q limit. Curves 3–4 of [Fig. 3](#) illustrate the PCEs corresponding to the LED voltages obtained using this scaling.

When considering the performance of the LED component alone ([Fig. 3](#), curves 2 and 4), all the PCE values clearly exceed the 100% efficiency threshold needed to reach the EL cooling regime. Depending slightly on whether the LED voltage is estimated using a resistive correction for the external voltage or a scaling law for the PD current, the LED efficiency peaks at values ranging between 106 and 115%. These estimates suggest that the best LEDs in the DDS structures already exceed the EL cooling threshold by an amount that is significantly larger than the error margin estimated based on the observed variations in the device characteristics. In principle, this also implies that our devices already exhibit thermophotonic cooling within the DDS cavity and that the direct measurement of an above-unity PCE and hence the experimental observation of EL cooling is within reach when the PD efficiency is improved or the surface recombination is suppressed. This could be accomplished, e.g., using established surface passivation methods and a more optimal PD structure or light extraction methods, providing light extraction efficiencies above the 70%–80% level.

In conclusion, we report results suggesting that the EL cooling barrier has been broken in the studied high efficiency GaAs LEDs, leading to thermophotonic cooling within the DDS cavity. Additionally, the studied devices exhibit a record for the quantum efficiency in the DDS aimed at the demonstration of high-power EL cooling and potentially the highest values for the directly measured quantum efficiency (0.70) and power conversion efficiency (up to 115%) of any GaAs based LED.

See [supplementary material](#) for the ABC-model and detailed information on the estimation of PD losses.

This project received funding from the Academy of Finland and the European Research Council (ERC) under the European Union's Horizon 2020 research and innovation programme (Grant Agreement No. 638173). We acknowledge the provision of facilities and the technical support from the Micronova Nanofabrication Centre at Aalto University.

REFERENCES

- ¹D. A. Bender, J. G. Cederberg, C. Wang, and M. Sheik-Bahae, *Appl. Phys. Lett.* **102**, 252102 (2013).
- ²P. Berdahl, *J. Appl. Phys.* **58**, 1369 (1985).
- ³M. Broell, P. Sundgren, A. Rudolph, W. Schmid, A. Vogl, and M. Behringer, "Light-emitting diodes: Materials, devices, and applications for solid state lighting XVIII," *Proc. SPIE* **9003**, 90030L (2014).
- ⁴K. Chen, T. P. Xiao, P. Santhanam, E. Yablonovitch, and S. Fan, *J. Appl. Phys.* **122**, 143104 (2017).
- ⁵R. S. DiMatteo, *AIP Conf. Proc.* **653**, 232–240 (2003).
- ⁶G. C. Dousmanis, C. W. Mueller, H. Nelson, and K. G. Petzinger, *Phys. Rev.* **133**, A316 (1964).
- ⁷H. Gauck, T. H. Gfroerer, M. J. Renn, E. A. Cornell, and K. A. Bertness, *Appl. Phys. A: Mater. Sci. Process.* **64**, 143 (1997).
- ⁸O. Heikkilä, J. Oksanen, and J. Tulkki, *J. Appl. Phys.* **105**, 093119 (2009).
- ⁹C. A. Hurni, A. David, M. J. Cich, R. I. Aldaz, B. Ellis, K. Huang, A. Tyagi, R. A. DeLille, M. D. Craven, F. M. Steranka et al., *Appl. Phys. Lett.* **106**, 031101 (2015).
- ¹⁰S. Karpov, *Opt. Quantum Electron.* **47**, 1293 (2015).
- ¹¹J. Oksanen and J. Tulkki, *J. Appl. Phys.* **107**, 093106 (7 p.) (2010).
- ¹²A. Olsson, J. Tiira, M. Partanen, T. Hakkarainen, E. Koivusalo, A. Tukiainen, M. Guina, and J. Oksanen, *IEEE Trans. Electron Devices* **63**, 3567 (2016).
- ¹³P. Pringsheim, *Z. Phys.* **57**, 739 (1929).
- ¹⁴I. Radevici, J. Tiira, T. Sadi, and J. Oksanen, *Semicond. Sci. Technol.* **33**(5), 05LT01 (2018).
- ¹⁵T. Sadi, P. Kivisaari, J. Tiira, I. Radevici, T. Haggren, and J. Oksanen, *Opt. Quantum Electron.* **50**, 18 (2018).
- ¹⁶P. Santhanam, D. J. Gray, and R. J. Ram, *Phys. Rev. Lett.* **108**, 097403 (2012).
- ¹⁷P. Santhanam, D. Huang, R. J. Ram, M. A. Remennyi, and B. A. Matveev, *Appl. Phys. Lett.* **103**, 183513 (2013).
- ¹⁸I. Schnitzer, E. Yablonovitch, C. Caneau, and T. J. Gmitter, *Appl. Phys. Lett.* **62**, 131 (1993).
- ¹⁹M. Sheik-Bahae and R. I. Epstein, *Nat. Photonics* **1**, 693 (2007).
- ²⁰J. Tauc, *Czech. J. Phys.* **7**, 275 (1957).
- ²¹I. E. Titkov, S. Y. Karpov, A. Yadav, V. L. Zerova, M. Zulonas, B. Galler, M. Strassburg, I. Pietzonka, H.-J. Lugauer, and E. U. Rafailov, *IEEE J. Quantum Electron.* **50**, 911 (2014).